Hashimoto Yaumasa (Orcid ID: 0000-0001-9363-6910)
Nagayasu Takeshi (Orcid ID: 0000-0002-0677-9364)

Alteration of the extracellular matrix and alpha-gal antigens in the rat lung scaffold reseeded using human vascular and adipogenic stromal cells

Running title: Extracellular matrix and alpha-gal antigen regeneration

Yasumasa Hashimoto[a,c], Tomoshi Tsuchiya[a,b], Ryoichiro Doi[a], Keitaro Matsumoto[a,c], Yoshikazu Higami[b,d], Eiji Kobayashi[e,f], Takeshi Nagayasu[a,c]

[a] Department of Surgical Oncology, Nagasaki University Graduate School of Biomedical Sciences
[b] Translational Research Center, Research Institute for Science & Technology, Tokyo University of Science, Chiba 278-8510, Japan
[c] Medical-Engineering Hybrid Professional Development Center, Nagasaki University Graduate School of Biomedical Sciences, Nagasaki 852-8501, Japan
[d] Laboratory of Molecular Pathology and Metabolic Disease, Faculty of Pharmaceutical Sciences, Tokyo University of Science, Chiba 278-8510, Japan
[e] Center for Development of Advanced Medical Technology, Jichi Medical University
[f] Department of Organ Fabrication, Keio University School of Medicine

Corresponding author:
Takeshi Nagayasu, MD, PhD
Department of Surgical Oncology, Nagasaki University Graduate School of Biomedical Sciences
1-7-1 Sakamoto, Nagasaki, JAPAN 852-8501
Telephone: +81-95-819-7304
Fax: +81-95-819-7306
Email: nagayasu@nagasaki-u.ac.jp

This article has been accepted for publication and undergone full peer review but has not been through the copyediting, typesetting, pagination and proofreading process which may lead to differences between this version and the Version of Record. Please cite this article as doi: 10.1002/term.2923

Summary

Regenerated organs are expected to solve the problem of donor-organ shortage in transplantation medicine. One approach to lung regeneration is to decellularize the organ and reseed it with selected cells. Advantage of the procedure includes reduced immunogenicity, since all cells can be theoretically replaced by autologous cells. However, little is known regarding the extracellular matrix (ECM) damage during decellularization and ECM reconstruction process in the organ regeneration. We aimed to evaluate ECM damage and reconstruction of the decellularized- recellularized rat lung, including the removal of alpha-gal xenoantigens. Rat lungs were perfused with sodium dodecyl sulfate and Triton X-100 via the pulmonary artery, after which the decellularized scaffold was reseeded with rat or human endothelial cells and adipose mesenchymal stem cells (ASCs). The ECM and alpha-gal antigen were evaluated using immunohistochemistry, western blotting, and a glycosaminoglycan assay. Alcian blue staining revealed increased production of proteoglycan following the addition of ASCs to the rat lung recellularized with rat lung microvascular endothelial cells. Glycosaminoglycan levels decreased in the decellularized lung and increased in the recellularized lung, especially in the ASC-treated group. Immunohistochemical expression of the alpha-gal protein was decreased to undetectable level in the decellularized lung tissue, and disappeared after recellularization with human cells. In western blot analysis, the bands of alpha-gal protein almost disappeared after recellularization with human cells. In conclusion, characteristics of the regenerated ECM might depend on the species and type of cells used for recellularization. Therefore, alpha-gal antigen might be eliminated after a prolonged culture, when using human cells.

Keywords: Decellularization, Extracellular matrix, Alpha-gal antigen, Lung regeneration, Tissue engineering

1. Introduction

Lung transplantation represents the only cure for intractable lung diseases, such as primary pulmonary hypertension, idiopathic interstitial pneumonia, and pulmonary lymphangioleiomyomatosis. However, donor organ shortages represent a crucial problem, and many patients die during the waiting period (Thomas, 2010). Engineered lungs represent a theoretical alternative for transplantation following end-stage lung failure. One approach is to decellularize the organ and reseed it with selected cells, ideally from the organ recipient. This approach has been tested for rodent, porcine, and human lungs, and may potentially lead to xenotransplantation in humans (Joseph, 2016). A xeno-organ scaffold can be used for lung-organ engineering, thereby offering novel alternatives for transplantation medicine.

An advantage of the decellularization approach includes reduction of immunogenicity of reconstructed organs, since all the cells can be replaced by autologous or isogenic cells, thus minimizing immunoreactivity (Maelene, 2014, Derek, 2014). The main disadvantage of this method is damage to the extracellular matrix (ECM), which is essential for the survival and proliferation of adherent cells (Tsuchiya, 2014). Since the lung consists of airways and vascular structures, damage to the airways can lead to failure of the ventilation system. Moreover, damage to vascular structures results in prompt thrombus formation. Therefore, many approaches have been tested for ECM preservation, including the optimization of both detergents as well as the decellularization process (Tsuchiya 2014, Collin, 2015). The

remaining xenoantigens in the decellularized ECM represent another crucial problem. The alpha-gal epitope (Galalpha1-3Galbeta1-(3)4GlcNAc-R) is a xenoantigen, which is synthesized in some glycolipids and glycoproteins of non-primate mammals and New World monkeys (Galili, 2001). However, the antigen is not found in primates including humans, who have lost the *GGTA1* gene during the evolutionary process. Removal of the alpha-gal epitope is a prerequisite for avoiding the hyper-acute rejection of untreated xenografts in human xenotransplantation (Maelene, 2014).

The aim of this study was to evaluate ECM damage and reconstruction during the decellularization and recellularization process. To investigate ECM damage and replacement during this process, we recellularized rat lungs using several types of rat or human cells. Decellularization decreased the number of ECM proteins containing rat lung-derived xenoantigens. Conversely, specific cells could secrete ECM proteins during the recellularization process, thus promoting ECM regeneration and leading to negligible levels of xenoantigens in the ECM.

2. Materials and methods

2.1.Organ harvest

All animal experiments were performed at Nagasaki University after being reviewed and approved by the Institutional Animal Care and Use Committee. Rat lung tissues were

obtained from young adult male rats (Fischer F344, 8–12 weeks old, CLEA, Japan, Tokyo). Rats were first anesthetized using an intraperitoneal injection of ketamine and isoflurane inhalation. After a sternal midline incision, further incisions were performed in both ventricles, and both lungs were perfused via the pulmonary artery with 50 mL phosphate buffered saline (PBS) containing heparin and sodium nitroprusside. The lungs (whose color changed to white) and trachea were extracted. The pulmonary artery, trachea, and left ventricle were cannulated, after which they were connected to a perfusion system and set in a bioreactor (Calle 2011, Doi 2017). All bioreactor components were provided from Cole-Parmer (Vernon Hills, IL).

2.2.Decellularization

We modified the mild decellularization technique described previously (Calle, 2016). All reagents were used in a 20-cm column under water pressure via a connection to the pulmonary artery. Thus, the lungs were gravity-perfused via the pulmonary artery at physiologically appropriate pulmonary artery pressures (below 20 mmHg). At first, the lungs were rinsed with 100 ml of PBS with calcium/magnesium containing heparin and sodium nitroprusside. Then, they were perfused with 500 ml of 0.0035% Triton X-100 (Sigma, St Louis, MO) in deionized water for 10 min and 250 ml of deoxyribonuclease reaction buffer containing magnesium chloride. Next, they were inflated with 10 ml of benzonase

endonuclease (90 U/mL) and incubated for 1 h. After rinsing with 500 ml of PBS containing 1 M NaCl, the lungs were decellularized with 0.01%, 0.05%, and 0.1% sodium dodecyl sulfate (SDS) in 0.5 L of deionized water. Furthermore, they were perfused with 100 ml of 0.5% Triton X-100 in deionized water. Finally, after a rinse with 2 L of PBS, the lungs were preventively perfused with 0.5 L of PBS containing antibiotics, such as 100 U/mL penicillin, 100 U/mL streptomycin (Invitrogen, Waltham, MA), and amphotericin B (Sigma), and stored at 4 °C until use. The whole decellularization process took almost 1 day.

2.3.Recellularization using rat and human cells

Recellularization was performed using adipose-derived stem cells (ASCs) and rat lung microvascular endothelial cells (RLMVECs: VEC Technologies, Rensselaer, NY). Rat ASCs were obtained from inguinal fat tissues of 8–12-week-old adult rats. Human ASCs were isolated from fat tissues provided by a 50-year-old woman after total mastectomy (Number: 18011513).

ASCs were isolated from the adipose tissues according to the procedure described by Zuk et al. (Zuk, 2001), with minor modifications. Briefly, the adipose tissue was digested with 0.001% collagenase (Celase®; Cytori, Tokyo Japan) at 37 °C for 30 min. After several cycles of shaking and centrifugation, the specimen was filtered through a nylon mesh. Mesenchymal cells were separated by centrifugation, and then re-suspended in OriCell Mesenchymal Stem

Cell Growth Medium (DS Pharma Biomedical, Osaka, Japan). The cells were cultured in 100-mm dishes for 14–18 days until they reached confluence. Isolated ASCs were used at passage 0 or 1 for recellularization.

The quality of ASCs was verified using cellular markers, such as the presence of CD44, CD73, and CD90, and the absence of CD11b/c, CD31, C34, and CD45, as previously reported (Bussolino, 1992). *In-vitro* tests, using appropriate culture conditions and supplements, confirmed the multi-lineage differentiation of adipose-derived mesenchymal stem cells towards the osteogenic, adipogenic, and chondrogenic lineages (data not shown). RLMVECs were purchased from VEC Technologies (Rensselaer, NY) and maintained in fibronectin-coated cell culture flasks (BD Biosciences) in microvascular EC growth medium (EGM-2MV, Lonza) with appropriate supplements (EGM-2MV BulletKit, Lonza). The culture medium was refreshed every 2 days. RLMVECs were passaged after reaching 80% confluence, using 0.25% trypsin-EDTA (Nacalai Tesque, Kyoto, Japan), and were used for recellularization. HUVECs were purchased from Lonza (C2517A; Lonza, Inc., Walkersville, MD, USA) and grown in EGM-2 medium containing human epidermal growth factor, vascular endothelial growth factor, R3-insulin-like growth factor-1, ascorbic acid, hydrocortisone, hFGF-β, heparin, FBS, and gentamicin/amphotericin-B (EGM-2 Bullet Kit; Lonza, Inc.). Lung recellularization was performed with modifications to published protocols (Doi, 2017). Forty million RLMVECs, with or without 10 million ASCs, were seeded via the

pulmonary artery (PA) and pulmonary vein (PV) into decellularized rat scaffolds. After 2 h in static culture, media were perfused from both PA and PV at 1 mL/h. One day later, after the PV cannula was released, the perfusion rate was switched to 4 mL/h. The medium was changed every 2 days until evaluation at 8 days. The regenerated lungs were prepared for histology, protein extraction, and frozen sectioning. Recellularization using human cells was achieved using human umbilical vein endothelial cells (HUVECs) and human ASCs.

2.4.Histological analysis

The lungs were fixed with 4% paraformaldehyde for at least 3 h at room temperature, paraffin embedded, and sectioned at a thickness of 5 μm. Analysis was performed with standard hematoxylin and eosin (H/E) staining. Masson's trichrome stain was used for collagen and muscle fiber staining, while Elastica Van Gieson (EVG) was used for elastin staining. Proteoglycans were visualized using Alcian blue staining.

Cells were counted at 40× magnification using H/E staining. Ten high-power view images from alveolar area of each lung were analyzed (n = 3). In each image, average cell number was calculated and compared across 5 groups.

2.5.Immunohistochemistry

After deparaffinization, antigen retrieval was performed by incubating sections in 10 mM citrate buffer (pH 6) at 95 °C for 40 min. Polyclonal anti-collagen I (NB600-408, Novus Biologicals, Littleton, CO), polyclonal anti-collagen IV (ab6586, Abcam, Tokyo, Japan), and polyclonal anti-laminin (ab74164; Abcam) antibodies were used as primary antibodies for overnight incubation at 4 °C for 16–24 h. After the secondary antibodies were applied, sections were washed thrice for 5 min. Finally, they were developed with 3,3-diaminobenzidine (DAB) for 5 min. For fibronectin staining, a polyclonal anti-fibronectin primary antibody (ab23751; Abcam) was used at a concentration of 1:1000 in signal stain antibody diluent (8112L; Cell Signaling Technology, Danvers, MS). After incubation with the secondary antibody, sections were washed thrice for 5 min and developed with DAB for 5 min. For the xenoantigen assay, sections were incubated with an alpha-gal primary monoclonal antibody (M86; Enzo, Tokyo, Japan) overnight at 4 °C for 16–24 h, followed by incubation with the secondary antibody, after which they were developed with DAB for 5 min.

For immunofluorescence staining, platelet endothelial cell adhesion molecule-1(PECAM/CD31, Santa Cruz) and NG-2 (Millipore) were used as the primary antibodies, as previously described (Doi, 2017). Briefly, antigen retrieval was performed by incubating the deparaffinized sections in 10 mM citrate buffer (pH 6) at 121 °C for 15 min. Sections were

then blocked with 1% BSA/0.3% Triton X-100 in PBS for 1 h and incubated overnight with primary antibodies at 4 °C. Next, sections were washed thrice with PBS and incubated in secondary antibodies for 1 h at room temperature, followed by three more washes in PBS. For ASC immunocytochemistry, cells in chamber slides were washed with PBS and fixed in methanol/acetone for 15 min at -20 °C. Slides were then blocked in PBS containing 1% BSA and incubated with either of the primary antibodies overnight at 4 °C. Slides were washed thrice with PBS and then incubated with secondary antibody for 1 h at room temperature, followed by three more washes in PBS. All stained sections were mounted in a mounting medium containing DAPI (Vector Laboratories, Burlingame, CA) and imaged using BZ-9000 BioRevo (Keyence) microscope. For quantitative analysis using immunostaining, ImageJ software (NIH) was used. Ten high-power view images (40× magnification) from the alveolar area in each immunostained lung were analyzed (n = 3). In each image, immunopositive areas over the threshold level were calculated, and divided by the number of alveoli in the field that were counted by particle analysis. Thus, protein expression per alveolus in each image could be validated.

2.6.Western blotting

An alpha-gal monoclonal antibody (M86; Enzo) and a β-actin antibody (ab1801; Abcam) were used as primary antibodies. After the addition of 500-1000 μL of RIPA/SDS buffer

containing protease inhibitors (08714; Nacalai Tesque, Japan), approximately 5-mm fresh-cut tissues were homogenized using a tissue homogenizer (Micro Smash MS-100R; TOMY SEIKO CO, Tokyo, Japan) at 5500 rpm for 100 s on ice. After lysis on ice for 30–60 min, the homogenized tissues were centrifuged at 10000 × g for 10 min at 4 °C. The supernatant (containing proteins) was used for western blotting. Concentration of the supernatant was measured using a protein assay kit (23225; Thermo Fisher, Tokyo, Japan). The proteins were fractionated using 7.5% SDS-polyacrylamide gel electrophoresis (SDS-PAGE) (4 μg/lane), following which, they were transferred and blotted onto a polyvinylidene difluoride (PVDF) membrane. After blocking with a blocking solution (20 mM Tris-HCl, pH, NaCl, 0.1% Tween-20, 0.6% polyvinylpyrrolidone) for 1 h, the membranes were incubated with primary antibodies overnight at 4 °C. After three washes in TBST, the membranes were incubated with horseradish peroxidase (HRP)-conjugated goat anti-mouse IgM antibodies (SC-2064; Santa Cruz Biotechnology, Santa Cruz, CA) for 1 h. The immunolabeled proteins were visualized using a LAS-3000 luminescent image analyzer and a Chemi-Lumi One Super kit (Nacalai Tesque).

2.7.Glycosaminoglycan (GAG) assay

The left lobe was used for the GAG assay. Lung tissues, cut in small pieces, were vacuum dried (VirTis; Benchtop K; CENTRAL SCIENTIFIC COMMERCE, Tokyo, Japan). After

lyophilization with a 1 mL papain solution, 5 mg of lyophilized tissues were incubated at 65 °C overnight (16–24 h) until most of the tissue was digested and dissolved. Sulfated GAGs were quantified using the Blyscan GAG Assay Kit (Biocolor, Carrickfergus, UK).

3. Results

3.1. Lung tissue engineering strategy

Native rat lung was cannulated at the PA, PV, and trachea for the infusion of SDS-based decellularization solutions (Fig. 1). Following lung decellularization, the acellular lung matrix was mounted into a biomimetic bioreactor, thereby allowing the seeding of cells. The gross appearance of the recellularized rat lung changed from white to a dark milky-white color after 8 days of culture owing to the seeded cells (2.4×10^7 for RLMVECs with or without 6×10^6 ASCs). The gross appearance was not different across the different cell combinations.

3.2.Histological findings

To assess decellularization and recellularization, we evaluated the following five groups (n = 3 animals/group): control group, decellularized group (decell group), (a) RLMVEC-seeded group (RLMVEC group), (b) rat RLMVECs with ASC-seeded group (RLMVEC-rASC group), and (c) human HUVECs with ASC-seeded group (HUVEC-hASC group).

When the rat lungs were subjected to decellularization using detergents, the decellularized scaffolds were completely devoid of any viable cell, as indicated by standard histological techniques (hematoxylin and eosin staining, Fig. 2A). After recellularization, endothelial cells lined the inside of the vessel walls in the RLMVEC group (Fig. 2B). In the RLMVEC-rASC group, spindle cells were observed within the alveolar walls, originating form rASCs (Fig. 2B). Moreover, the HUVEC-hASC group showed a similar distribution of seeded cells as in the RLMVEC-rASC group (Fig. 2B). Double immunofluorescence staining of the endothelial marker CD31 and pericyte marker NG-2 showed the seeded cells to be positive for CD31 in the RLMVEC group. At day 8 of culture, in addition, NG-2-positive cells were seen in both RLMVEC-rASC and HUVEC-hASC groups (Fig. 2C). Comparison of cell count per area in each lung showed the attached cells to be different across the groups analyzed (Fig. 2E).

Using Masson's trichrome stain, we showed that the density of collagen fibrils was preserved after decellularization and the densities in each group were similar after recellularization (Fig. 3A-3E). Moreover, EVG staining indicated wavy elastic fibers in the vascular wall, while the alveolar septum was dyed dark and collagen was dyed light red (Fig. 3F-3J). However, there was no obvious difference across the five groups. The proteoglycans in the alveolar septum were dyed light blue when using Alcian blue staining. Interestingly, the RLMVEC-rASC and HUVEC-hASC groups displayed clear proteoglycan staining in the perivascular area and alveolar septa (Fig. 3N and 3O), in contrast to the RLMVEC-only

group (Fig. 3M).

3.3.Immunohistochemistry of matrix proteins

Collagen is the most abundant protein within the mammalian ECM (van der Rest, 1991). Collagen I is the major structural protein present in tissues while collagen IV forms a complex branched network and is largely present within the basement membrane of most vascular structures and within tissues that contain an epithelial cell component. The immunohistochemical staining of collagen I and IV revealed that large vessels and alveolar septa were immunopositive in all of the five groups. However, consistent with the results observed for Masson's trichrome staining, there was no clear difference among the five groups (Fig. 4A and 4B).

Fibronectin and laminin play a prominent role in the formation and maintenance of vascular structures and represent complex adhesion proteins found in the ECM, especially within the basement membrane (Sannes, 1993). Immunohistochemical staining of fibronectin revealed that large vessels and alveolar septa were immunopositive in all groups (Fig. 4C). However, no clear difference was apparent among the five groups. Similar results were obtained for laminin staining (Fig. 4D). Important ECM proteins, such as laminin and fibronectin, were retained even after decellularization and recellularization. No significant difference was found across the 5 groups upon quantitative analysis using ImageJ (Fig. 4E).

3.4.Comparison of proteoglycan levels in rat lungs

GAGs help to control the macromolecular and cellular movement across the basal lamina (van der Rest, 1991). Proteoglycans represent one component of the extracellular matrix and consist of many GAGs. The GAGs of proteoglycans affect the stretching and folding pattern of the fibers. To assess the GAG content in all five groups, we used the GAG assay kit. GAG content in the decell group was significantly decreased compared to that in the control group (Fig. 5). Although the GAG content in the rRLMVEC group was 7.2-fold higher than that in the decell group ($p = 0.78$), it represented only 10.1% of the GAG content of control group ($p < 0.0001$). On the other hand, GAG levels in the rRLMVEC-ASC and HUVEC-ASC groups recovered to 54.1% and 32.6%, respectively, of that in the control group.

3.5. Comparison of alpha-gal antigen expression among native, decellularized, and recellularized rat lungs

To determine whether decellularization and recellularization procedures can reduce the levels of glycoproteins in the ECM, we evaluated the expression of alpha-gal epitopes in the native, decellularized, and recellularized rat lung using human cells. The alpha-gal epitopes were strongly expressed on the cell membrane of both endothelial and alveolar epithelial cells in the native rat lung (Fig. 6A). On the other hand, their expression was undetectable in the decellularized and recellularized rat lungs (Fig. 6A). Using western blotting, multiple bands

were observed in the native rat lung, indicating that alpha-gal epitopes adhere to many proteins in the lung (Fig. 6B). In the decellularized rat lung, only two bands were observed, suggesting that alpha-gal epitopes are still present and adhere to the remaining ECM proteins after detergent digestion. Conversely, in the group that was recellularized using human cells, these bands almost disappeared. The cell-component protein beta-actin disappeared after decellularization and reappeared after recellularization (Fig. 6C).

4. Statistical Methods

Numerical values are presented as the mean ± SD. Statistical significance was evaluated using the unpaired Student's t-test for comparisons between two groups, and Kruskal-Wallis test for comparisons between three groups. All statistical analyses were performed using the SPSS software package. Statistical significance has been reported at all relevant instances accordingly.

5. Discussion

Advantages of using the decellularization method in regenerative medicine lie in the preservation of the ECM (Balestrini, 2016) and antigen removal (Wong, 2014; Cissell, 2014). However, reseeded cells can produce their own ECM. The main purpose of this study was to observe the changes in ECM during the decellularization and recellularization processes in a

rat lung scaffold. Our immunohistochemistry results showed that some ECM proteins in the decellularized scaffold are comparable to those in the native rat lung. Calle et al. reported that a mild decellularization technique can result in near-native retention of the ECM (Calle, 2016). The modified mild decellularization technique in the present study might affect the preservation of major ECM proteins.

However, in the GAG assay, the glycosaminoglycan content decreased significantly in the decellularized scaffold. Preservation of glycosaminoglycans (GAGs) during the decellularization process appears to be important, since GAGs play a key role in the mechanical integrity of the lung (Petersen, 2012; Stabler, 2015), and also help to control the macromolecular and cellular movements across the basal lamina (Stabler, 2015). Interestingly, in our present study, the GAG levels partially recovered, following reseeding with RLMVECs and ASCs, to levels significantly higher than that in the RLMVEC-seeded group. Prakash et al. mentioned that in the recellularization of a decellularized scaffold, mesenchymal stem cells (MSCs) play key roles in the secretion of several growth factors, immune modulators, and other key factors (Prakash, 2015). Further, Stabler et al. had proposed that the cells used for reseeding the decellularized scaffold can regenerate the damaged ECM in the decellularized lung through their innate capacity to produce their own ECM (Stabler, 2015). In other words, cells such as endothelial cells, MSCs, and pericytes may remodel and rebuild the ECM and further generate capillaries. Our current results

strongly support their hypothesis. The present results indicated that reseeded cells can regenerate the ECM; characteristics and amount of replaced ECM might depend on the species and the type of cells used for recellularization. If human cells are used, the decellularized rat ECM may convert into a human ECM. This theory led us to believe that if a xeno-lung scaffold can be recellularized by human cells, the regenerated ECM might adapt to the human internal environment and thus engineered organs may attain their structural and functional integrity after transplantation into humans. Considering that distinguishing between human and animal ECM is technically quite difficult at present, this theory should be substantiated by demonstrating the species/origin of the deposited ECM post seeding, in future.

Our second objective was to determine whether our decellularization protocol can remove xenoantigens from the rat lung. Therefore, we focused on the removal of alpha-gal epitopes. Although the alpha-gal antigen was immunohistochemically undetectable in the decellularized lung, two bands were still observed using western blot analysis. This discrepancy may be explained by the differences in the total protein levels between the decellularized and recellularized lung. The total protein content of the decellularized lung is 3.3-fold lower than that of the whole native rat lung, and for equal amounts of loaded proteins, bands derived from the decellularized rat lung may appear more intense. More interestingly, the alpha-gal bands observed in samples from recellularized lungs when using

human cells were hardly detectable, even on a western blot. This indicates that recellularization by human cells can attenuate the alpha-gal antigen concentration to undetectable levels and minimize the immunoreactivity to xenoantigens after the transplantation of engineered lungs. For decellularized simple tissues such as heart valves (Naso, 2011), blood vessels (Böer, 2011), cartilage (Elder, 2009), bone (Woods, 2005), and skin (Xu, 2009), various decellularization methods can remove not only cellular components but also xenoantigens including alpha-gal epitopes. Naso et al. (Naso, 2011) had reported that alpha-gal was no longer detectable in pig heart valves after TriCol treatment. Moreover, Nam et al. (Nam, 2012) demonstrated that α-galactosidase treatment and decellularization could effectively remove alpha-gal epitopes from the bovine pericardium. However, it is unlikely that cellular component and various antigens will be removed from complex tissues such as the lung, liver, and kidneys. According to our results, the complete removal of alpha-gal epitopes was not attained. However, considering out results obtained from recellularized lungs, using human cells, elimination of alpha-gal epitopes might be achieved by culturing the lungs over a long time. As a result, immunogenicity of the ECM might be eliminated by the ECM itself when recellularization is performed with the patient's own cells. In addition, the use of organs from alpha 1,3-galactosyltransferase knockout animals may aid the decellularization process, leading to a more complete removal of alpha-gal antigens.

A limitation of our study is that we only measured the levels of glycosaminoglycans but not those of other ECM proteins. In addition, we did not show that the rat ECM is completely replaced by the human ECM. Mass spectrometry-based analyses would be necessary in order to distinguish the different species from which the ECM had originated.

6. Conclusion

In conclusion, our results indicate that most of the ECM was preserved and some ECM could be replaced during the decellularization and recellularization processes, especially as proteoglycans are produced by ASCs. During this process, the alpha-gal epitope levels are diminished after recellularization when using human cells. Moreover, these epitopes may be eliminated after a long time in culture. If the reseeded cells can regenerate, maintain tissue integrity, and rebuild the xeno-scaffold into a human ECM, this method may prove more reliable for lung tissue engineering.

Acknowledgments

We gratefully acknowledge the technical support of Toshimitsu Komatsu (Department of Pathology, Graduate School of Biomedical Sciences, Nagasaki University, Nagasaki) and Hitoshi Takahashi (Department of Dermatology, Shimane University Faculty of Medicine, Shimane). This work was supported by a Grant-in-Aid for Scientific Research from the Japan

Society for the Promotion of Science (T.T., grant numbers 23592067 and 15H04944).

We would like to thank Editage (www.editage.jp) for English language editing.

Disclosures

The authors declare that there are no conflicts of interest.

References

Balestrini, J. L., Gard, A. L., Gerhold, K. A., Wilcox, E. C., Liu, A., Schwan, J., Le, A. V., Baevova, P., Dimitrievska, S., Zhao, L., Sundaram, S., Sun, H., Rittié, L., Dyal, R., Broekelmann, T. J., Mecham, R. P., Schwartz, M. A., Niklason, L. E., & White, E. S. (2016). Comparative biology of decellularized lung matrix: Implications of species mismatch in regenerative medicine. Biomaterials, 102, 220–230. *doi*: **10.1016/j.biomaterials.2016.06.025**

Böer, U., Lohrenz, A., Klingenberg, M., Pich, A., Haverich, A., & Wilhelmi, M. (2011). The effect of detergent-based decellularization procedures on cellular proteins and immunogenicity in equine carotid artery grafts. Biomaterials, 32, 9730–9737. *doi*: **10.1016/j.biomaterials.2011.09.015**

Bussolino, F., Di Renzo, M. F., Ziche, M., Bocchietto, E., Olivero, M., Naldini, L., Gaudino, G., Tamagnone, L., Coffer, A., & Comoglio, P. M. (1992). Hepatocyte growth factor is a potent angiogenic factor which stimulates endothelial cell motility and growth. The Journal of Cell Biology, 119, 629–641. *doi*: **10.1083/jcb.119.3.629**

Calle, E. A., Hill, R. C., Leiby, K. L., Le, A. V., Gard, A. L., Madri, J. A., Hansen, K. C., &

Niklason, L.E. (2016). Targeted proteomics effectively quantifies differences between native lung and detergent-decellularized lung extracellular matrices. Acta Biomaterialia, 46, 91–100. *doi*: **10.1016/j.actbio.2016.09.043**

Calle, E. A., Petersen, T. H., & Niklason, L. E. (2011) Procedure for lung engineering. Journal of Visualized Experiments, (49), 2651. *doi*: **10.3791/2651**

Cavalcante, F. S. A., Ito, S., Brewer, K., Sakai, H., Alencar, A. M., Almeida, M. P., Andrade, J. S., Majumdar, A., Ingenito, E. P., & Suki, B. (2005). Mechanical interactions between collagen and proteoglycans: implications for the stability of lung tissue. Journal of Applied Physiology, 98, 672–679. *doi*: **10.1152/japplphysiol.00619.2004**

Cissell, D. D., Hu, J. C., Griffiths, L. G., & Athanasiou, K. A. (2014). Antigen removal for the production of biomechanically functional, xenogeneic tissue grafts. Journal of Biomechanics, 47, 1987–1996. *doi*: **10.1016/j.jbiomech.2013.10.041**

Doi, R., Tsuchiya, T., Mitsutake, N., Nishimura, S., Matsuu-Matsuyama, M., Nakazawa, Y., Ogi, T., Akita, S., Yukawa, H., Baba, Y., Yamasaki, N., Matsumoto, K., Miyazaki, T., Kamohara, R., Hatachi, G., Sengyoku, H., Watanabe, H., Obata, T., Niklason, L. E., & Nagayasu, T. (2017). Transplantation of bioengineered rat lungs recellularized with endothelial and adipose-derived stromal cells. Scientific Reports, 7, 8447. *doi*: **10.1038/s41598-017-09115-2**

Elder, B. D., Eleswarapu, S. V., & Athanasiou, K. A. (2009). Extraction techniques for the

decellularization of tissue engineered articular cartilage constructs. Biomaterials, 30, 3749–3756. *doi*: **10.1016/j.biomaterials.2009.03.050**

Galili, U. (2001). The α-gal epitope (Galα1-3Galβ1-4GlcNAc-R) in xenotransplantation. Biochimie, 83, 557–563.

Nam, J., Choi, S. Y., Sung, S. C., Lim, H. G., Park, S. S., Kim, S. H., & Kim, Y. J. (2012). Changes of the structural and biomechanical properties of the bovine pericardium after the removal of α-gal epitopes by decellularization and α-galactosidase treatment. The Korean Journal of Thoracic and Cardiovascular Surgery, 45, 380–389. *doi*: **10.5090/kjtcs.2012.45.6.380**

Naso, F., Gandaglia, A., Iop, L., Spina, M., & Gerosa, G. (2011). First quantitative assay of alpha-Gal in soft tissues: Presence and distribution of the epitope before and after cell removal from xenogeneic heart valves. Acta Biomaterialia, 7, 1728–1734. *doi*: **10.1016/j.actbio.2010.11.030**

Petersen, T. H., Calle, E. A., Colehour, M. B., & Niklason, L. E. (2012). Matrix composition and mechanics of decellularized lung scaffolds. Cells, Tissues, Organs, 195, 222–231. *doi*: **10.1159/000324896**

Petersen, T. H., Calle, E. A., Zhao, L., Lee, E. J., Gui, L., Raredon, M. B., Gavrilov, K., Yi, T., Zhuang, Z. W., Breuer, C., Herzog, E., & Niklason, L. E. (2010). Tissue-engineered lungs for in vivo implantation. Science, 329, 538–541. *doi*: **10.1126/science.1189345**

Platz, J., Bonenfant, N. R., Uhl, F. E., Coffey, A. L.,

McKnight, T., Parsons, C., Sokocevic, D., Borg, Z. D., Lam, Y. W., Deng, B., Fields, J. G.,

DeSarno, M., Loi, R., Hoffman, A. M., Bianchi, J., Dacken, B., Petersen, T., Wagner, D. E., &

Weiss, D. J. (2016). Comparative decellularization and recellularization of wild-type and

alpha 1,3 galactosyltransferase knockout pig lungs: A model for ex vivo xenogeneic lung

bioengineering and transplantation. Tissue Engineering Part C Methods, 22, 725–739. *doi*:

10.1089/ten.TEC.2016.0109

Prakash, Y. S., Tschumperlin, D. J., & Stenmark, K. R. (2015). Coming to terms with tissue

engineering and regenerative medicine in the lung. American Journal of Physiology: Lung

Cellular and Molecular Physiology, 309, L625-638. *doi*: **10.1152/ajplung.00204.2015**

Sannes, P. L., Burch, K. K., Khosla, J., McCarthy, K. J., & Couchman, J. R. (1993).

Immunohistochemical localization of chondroitin sulfate, chondroitin sulfate proteoglycan,

heparan sulfate proteoglycan, entactin, and laminin in basement membranes of postnatal

developing and adult rat lungs. American Journal of Respiratory Cell and Molecular Biology,

8, 245–251. *doi*: **10.1165/ajrcmb/8.3.245**

Stabler, C. T., Lecht, S., Mondrinos, M. J., Goulart, E., Lazarovici, P., & Lelkes, P. I. (2015).

Revascularization of decellularized lung scaffolds: principles and progress.

American Journal of Physiology: Lung Cellular and Molecular Physiology, 309, L1273–

L1285. *doi*: **10.1152/ajplung.00237.2015**

Tsuchiya, T., Balestrini, J. L., Mendez, J., Calle, E. A., Zhao, L., & Niklason, L. E. (2014). Influence of pH on extracellular matrix preservation during lung decellularization. Tissue Engineering Part C Methods, 20, 1028–1036. *doi*: **10.1089/ten.TEC.2013.0492**

Tsuchiya, T., Sivarapatna, A., Rocco, K., Nanashima, A., Nagayasu, T., & Niklason, L. E. (2014). Future prospects for tissue engineered lung transplantation. Organogenesis, 10, 197–207. *doi*: **10.4161/org.27846**

van der Rest, M. & Garrone, R. (1991). Collagen family of proteins. FASEB J., 5, 2814–2823.

Wong, M. L. & Griffiths, L. G. (2014). Immunogenicity in xenogeneic scaffold generation: Antigen removal vs. decellularization. Acta Biomaterialia, 10, 1806–1816. *doi*: **10.1016/j.actbio.2014.01.028**

Woods, T. & Gratzer, P. F. (2005). Effectiveness of three extraction techniques in the development of a decellularized bone-anterior cruciate ligament-bone graft. Biomaterials, 26, 7339–7349. *doi*: **10.1016/j.biomaterials.2005.05.066**

Xu, H., Wan, H., Zuo, W., Sun, W., Owens, R. T., Harper, J. R., Ayares, D. L., & McQuillan, D. J. (2009). A porcine-derived acellular dermal scaffold that supports soft tissue regeneration: removal of terminal galactose-alpha-(1,3)-galactose and retention of matrix structure. Tissue Engineering Part A, 15, 1807–1819. *doi*: **10.1089/ten.tea.2008.0384**

Zuk, P.A., Zhu, M., Mizuno, H., Huang, J., Futrell, J. W., Katz, A. J., Benhaim, P., Lorenz, H.

P., & Hedrick, M. H. (2001). Multilineage cells from human adipose tissue: Implications for cell-based therapies. Tissue Engineering, 7, 211–228. *doi*: **10.1089/107632701300062859**

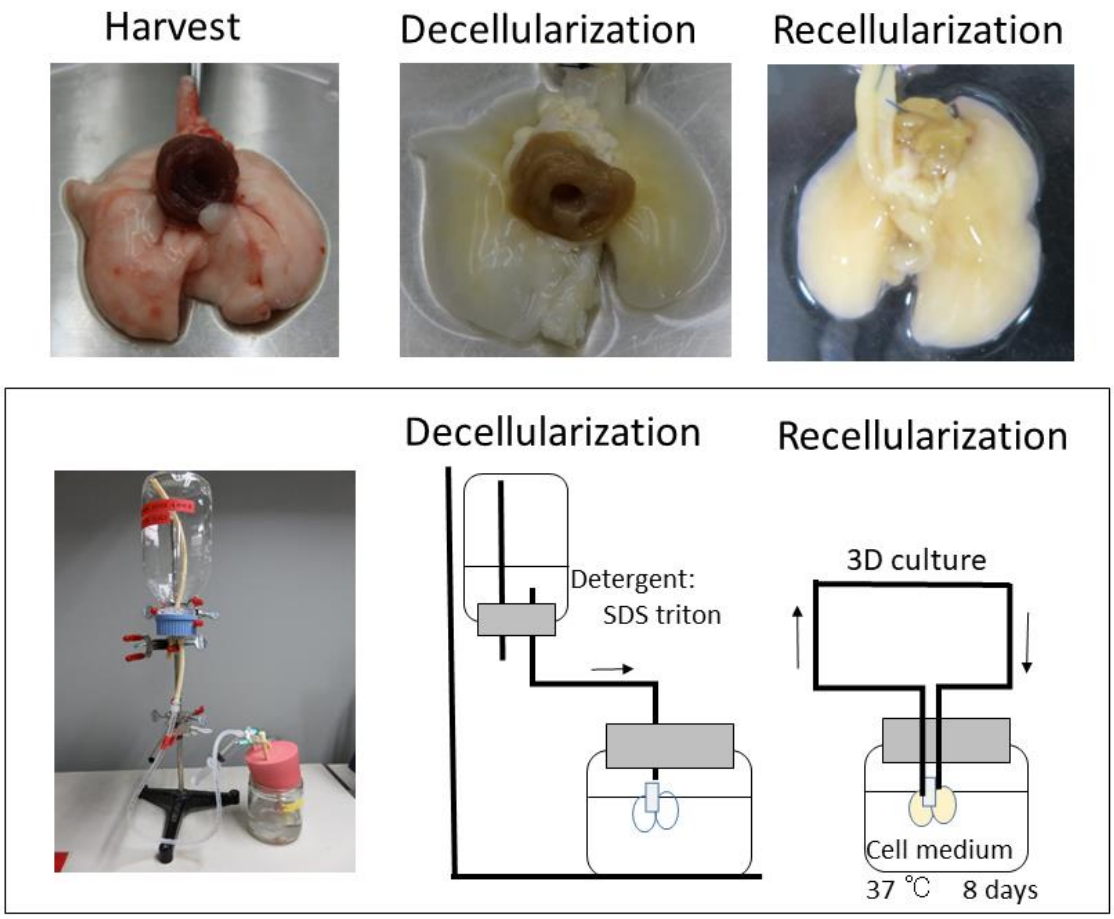

Fig. 1 Schematic protocol for lung organ regeneration for use in allotransplantation or xenotransplantation.

Photograph of native, decellularized, and recellularized rat lung. The decellularized rat lung was generated using various detergents, such as SDS and Triton X-100. All reagents were used in a 20-cm column under water pressure via a connection to the pulmonary artery. Recellularization was performed using adipose-derived stem cells (ASCs) and rat lung microvascular endothelial cells (RLMVECs). Recellularization using human cells was performed using human umbilical vein endothelial cells (HUVECs), and human ASCs incubated in a bioreactor at 37 °C for 8 days.

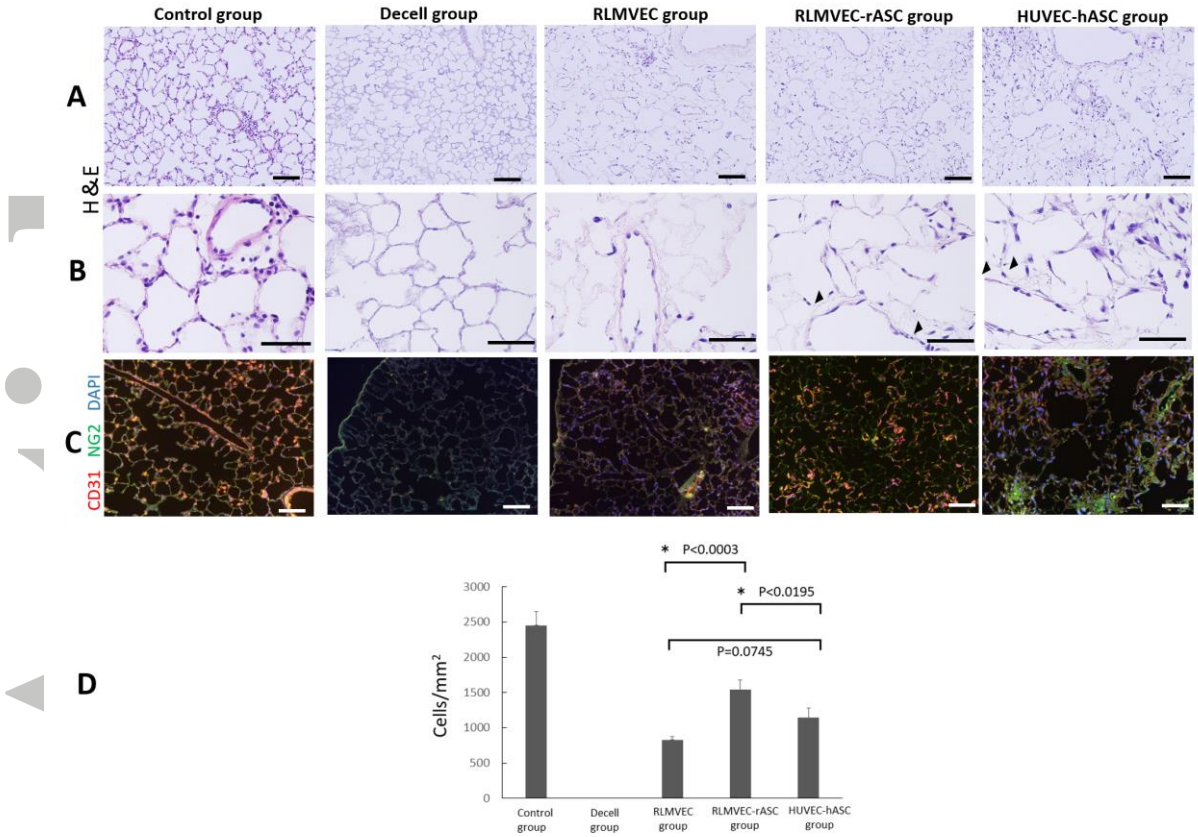

Fig. 2 H&E staining and immunofluorescence of thin sections from decellularized and recellularized lungs.

100x magnification views of the control, decellularized, and recellularized lungs, including the RLMVEC, RLMVEC–rASC, and HUVEC–hASC groups (A). 400x magnification views of the control, decellularized, and recellularized lungs, including the RLMVEC, RLMVEC–rASC, and HUVEC–hASC groups. When rat lungs were subjected to detergent decellularization, the decellularized scaffolds were completely devoid of any viable cells, as indicated by standard histological techniques. No intact nuclei are observed in decellularized lungs compared to the native lung control. Endothelial cells line the inside of the vascular walls in all recellularized groups. Few cells in the alveolar septa in the RLMVEC group. Spindle cells originating from rASCs in the RLMVEC-rASC group, observed among the alveolar walls. Similar distribution of seeded cells between the HUVEC-hASC and the RLMVEC-rASC groups (B). Double immunofluorescence staining of the endothelial marker CD31 (red) and pericyte marker NG-2 (green). Note that CD31-positive cells were observed in RLMVEC seeded lungs. NG-2-positive cells were observed in ASC- seeded groups, but not in RLMVEC-seeded lung (C). Cell counts of decellularized and recellularized lung per area. Scale bars: 100 μm：A, 50 μm：B, 50 μm：C. RLMVECs, rat lung microvascular endothelial cells; ASCs, adipose-derived stem cells; HUVECs, human umbilical vein endothelial cells (D).

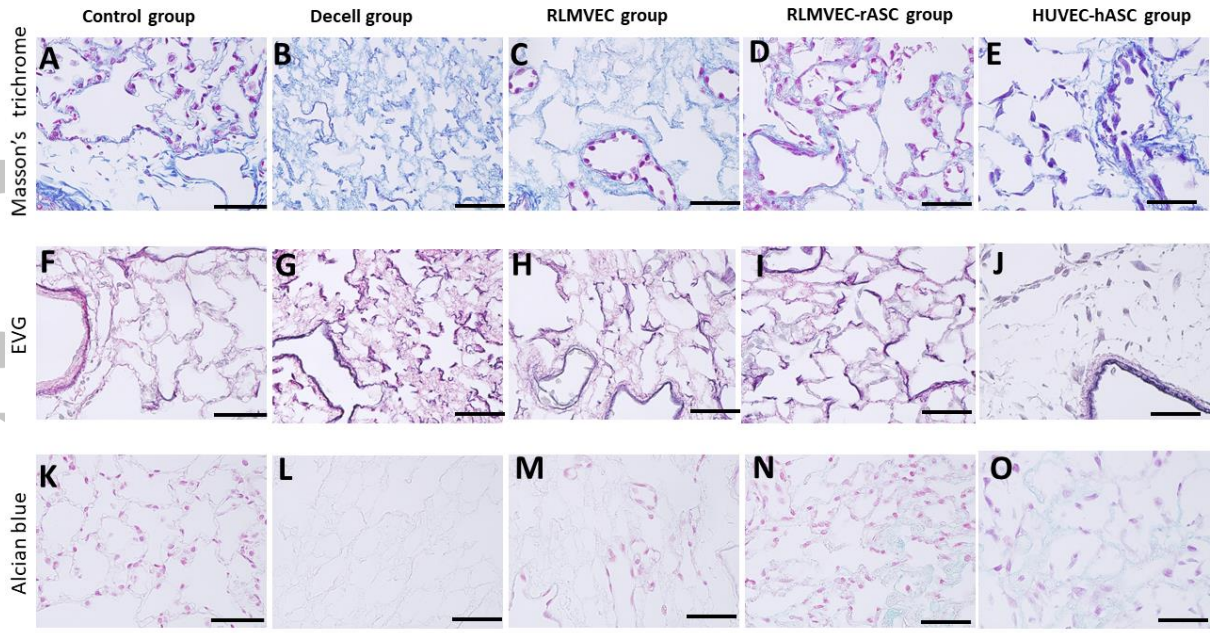

Fig. 3 Staining for collagen fibrils, elastic fibers, and proteoglycans before and after recellularization

Masson's trichrome staining showing that the density of collagen fibrils is preserved after decellularization and the densities in each group did not increase after recellularization (A-E). Elastic fibers assessed by Elastica Van Gieson (EVG) staining showing no differences between the groups: wavy elastic fibers in the vascular wall and alveolar septum were dyed dark, and collagen was dyed light red (F-J). Alcian blue staining, showing proteoglycans in the alveolar septum dyed in light blue. The RLMVEC-rASC and HUVEC-hASC groups show clear proteoglycan staining in the perivascular area and alveolar septa (N and O). Lack of staining in the RLMVEC group (M). Scale bars: 50 μm RLMVECs, rat lung microvascular endothelial cells; ASCs, adipose-derived stem cells; HUVECs, human umbilical vein endothelial cells

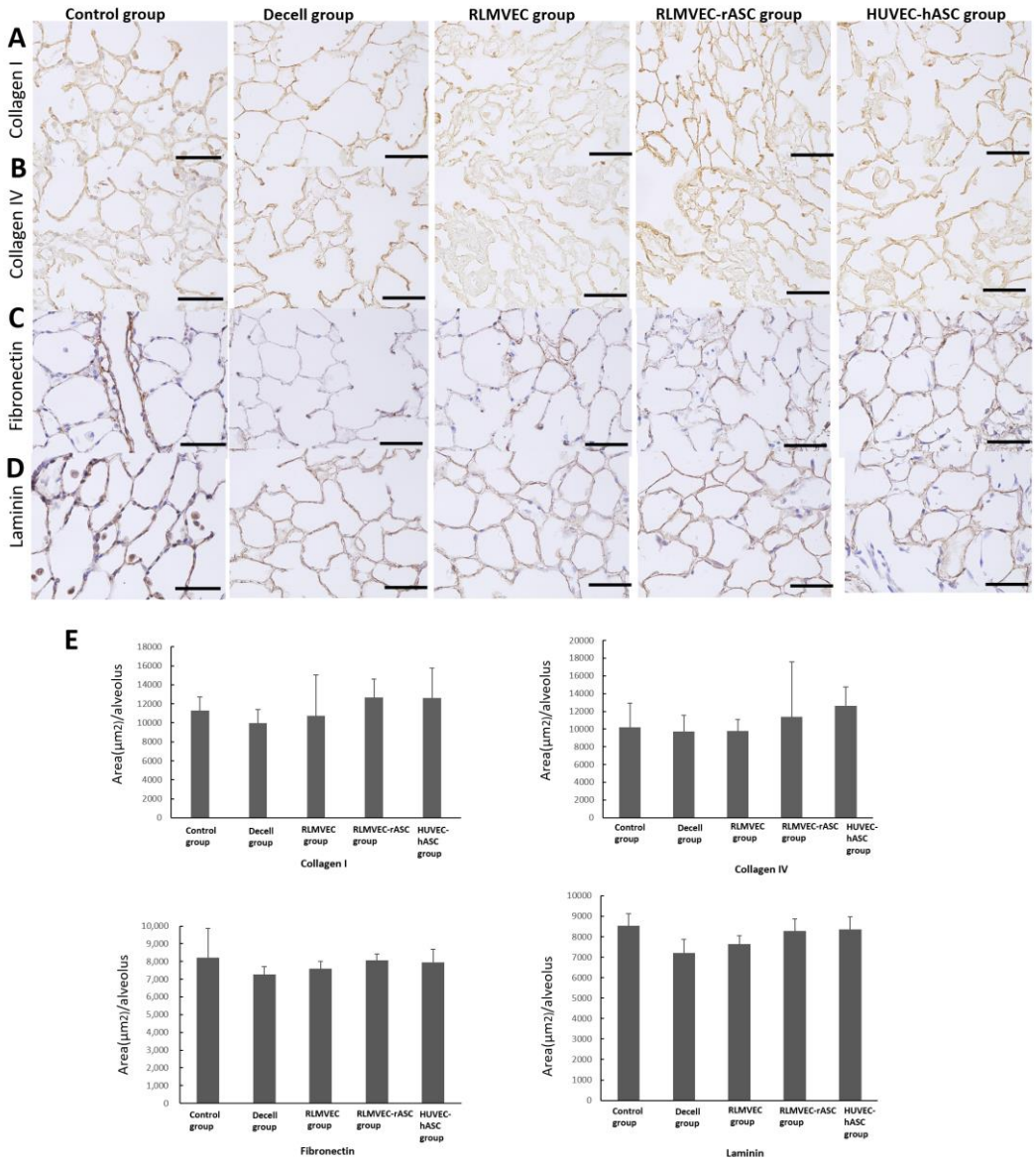

Fig. 4 Immunohistochemical staining of ECMs in the decellularized and recellularized groups

Immunohistochemical staining of collagen I (A) and IV (B), fibronectin (C), and laminin (D), revealing large immunopositive vessels and alveolar septa in all groups. Quantitative image analysis showed no difference between the groups (E). Scale bars: 50 μm.

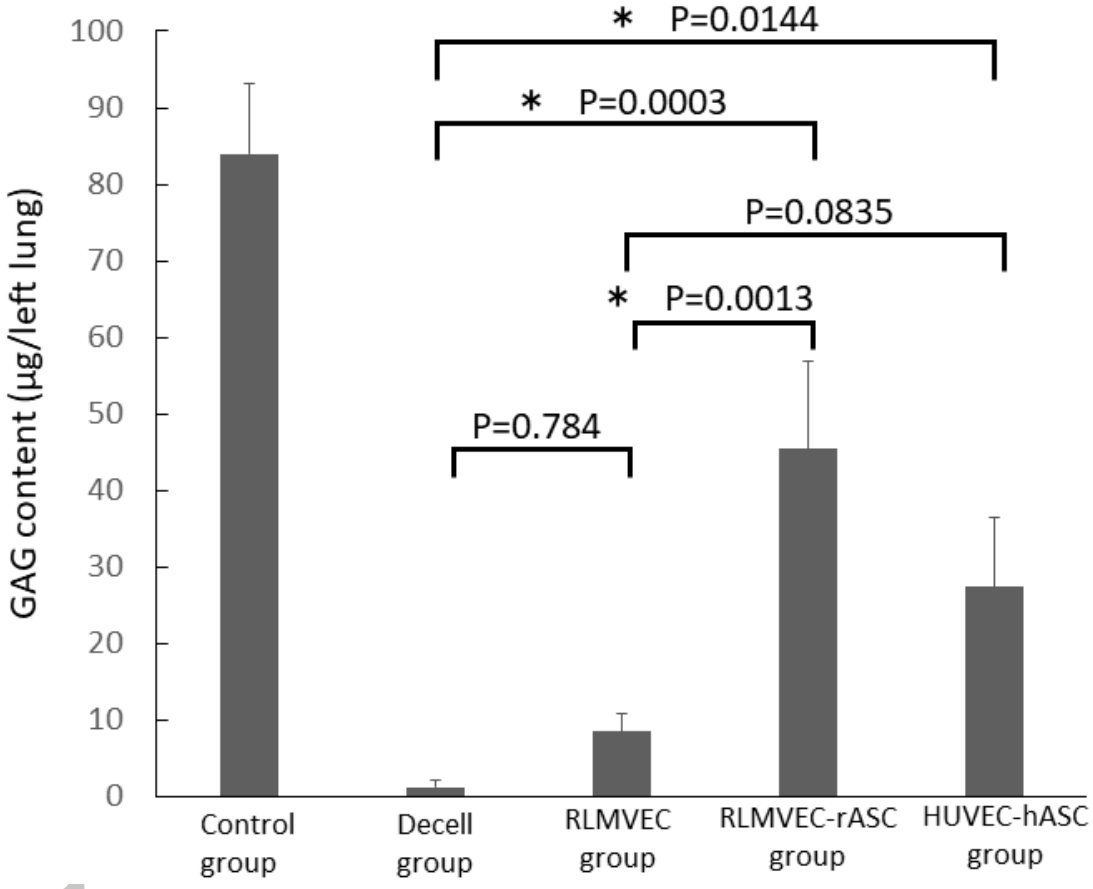

Fig. 5 GAG levels in decellularized and recellularized lungs

GAG content in the control, decell, RLMVEC, RLMVEC-ASC, and HUVEC-ASC groups. Decell, decellularized; RLMVECs, rat lung microvascular endothelial cells; ASCs, adipose-derived stem cells; HUVECs, human umbilical vein endothelial cells

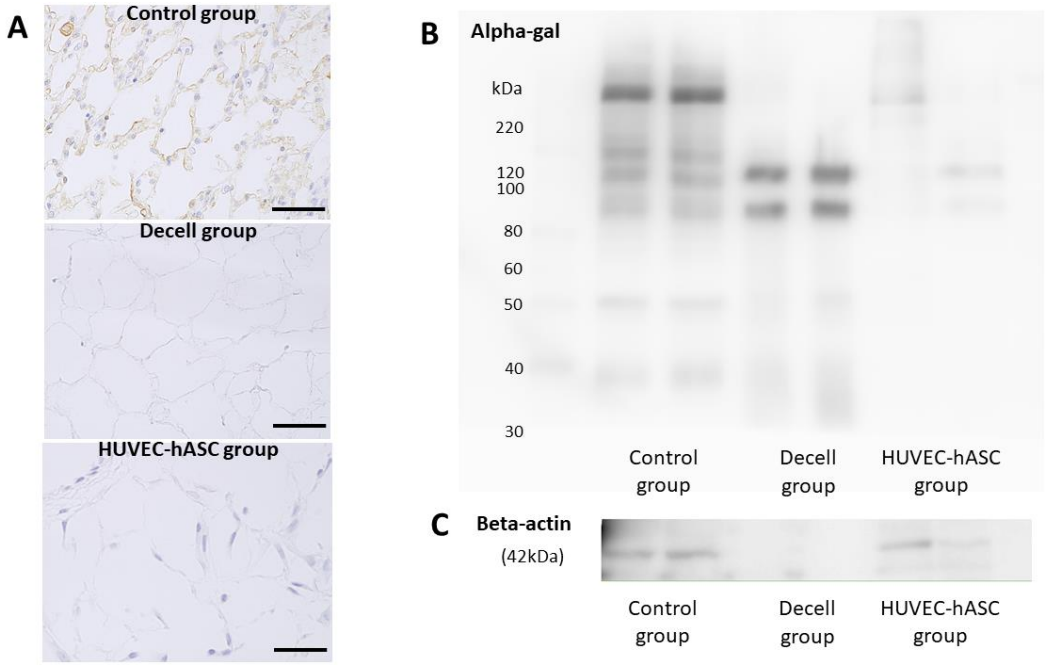

Fig. 6 Expression of alpha-gal epitopes in the native, decellularized, and recellularized rat lung using human cells

Immunohistochemical staining of alpha-gal epitope showed immune-positive rat native lung (Control group), but immune-negative decellularized rat lung scaffold (Decell group). Note that HUVEC and hASC reseeded rat lungs (HUVEC-hASC group) were also immune-negative for alpha-gal epitope (A). In western blot analysis of alpha-gal protein, 90- and 120-kDa bands were retained after decellularization, but very faintly detected in the recellularized rat lung when using human cells (B). In western blot analysis of beta-actin, 42-kDa bands were not present in decellularized group, but existed in the control and recellularized groups (C). Scale bars: 50 μm. Decell, decellularized; ASC, adipose-derived stem cell; HUVEC, human umbilical vein endothelial cell.